



A Journal of the Gesellschaft Deutscher Chemiker

# Angewandte Chemie

GDCh

International Edition

[www.angewandte.org](http://www.angewandte.org)

## Accepted Article

**Title:** Restraining Cancer Cells by Dual-Metabolic Inhibitions with a Mitochondrion-Targeted Platinum(II) Complex

**Authors:** Kun Wang, Chengcheng Zhu, Yafeng He, Zhenqin Zhang, Wen Zhou, Nafees Muhammad, Yan Guo, Xiaoyong Wang, and Zijian Guo

This manuscript has been accepted after peer review and appears as an Accepted Article online prior to editing, proofing, and formal publication of the final Version of Record (VoR). This work is currently citable by using the Digital Object Identifier (DOI) given below. The VoR will be published online in Early View as soon as possible and may be different to this Accepted Article as a result of editing. Readers should obtain the VoR from the journal website shown below when it is published to ensure accuracy of information. The authors are responsible for the content of this Accepted Article.

**To be cited as:** *Angew. Chem. Int. Ed.* 10.1002/anie.201900387  
*Angew. Chem.* 10.1002/ange.201900387

**Link to VoR:** <http://dx.doi.org/10.1002/anie.201900387>  
<http://dx.doi.org/10.1002/ange.201900387>

## COMMUNICATION

# Restraining Cancer Cells by Dual-Metabolic Inhibitions with a Mitochondrion-Targeted Platinum(II) Complex

Kun Wang,<sup>[a]</sup> Chengcheng Zhu,<sup>[a]</sup> Yafeng He,<sup>[a]</sup> Zhenqin Zhang,<sup>[a]</sup> Wen Zhou,<sup>[a]</sup> Nafees Muhammad,<sup>[a]</sup> Yan Guo,<sup>[a]</sup> Xiaoyong Wang,<sup>\*[b]</sup> and Zijian Guo<sup>\*[a]</sup>

**Abstract:** Cancer cells usually adapt metabolic phenotypes to chemotherapeutics. A defensive strategy against this flexibility is to modulate signaling pathways relevant to cancer bioenergetics. A triphenylphosphonium-modified terpyridine platinum(II) complex (TTP) was designed to inhibit thioredoxin reductase (TrxR) and multiple metabolisms of cancer cells. TTP exhibits enhanced cytotoxicity against cisplatin-insensitive human ovarian cancer cells in a caspase-3-independent way, and shows preferential inhibition on mitochondrial TrxR. The morphology and function of mitochondria are severely damaged, and the levels of mitochondrial and cellular reactive oxygen species are decreased. As a result, TTP exerts strong inhibition to both mitochondrial and glycolytic bioenergetics, inducing cancer cells to enter into a hypometabolic state.

Mitochondrial metabolism has long been misunderstood as a bystander in the oncogenic process of rapidly proliferating cells;<sup>[1,2]</sup> whereas emerging evidences reveal that it is essential for tumorigenesis in providing metabolic intermediates through anabolism and catabolism.<sup>[3,4]</sup> Many metal complexes have been reported to target mitochondria and damage mitochondrial metabolism;<sup>[5,6]</sup> however, the effect is discounted due to the alteration of metabolic phenotypes from oxidative phosphorylation to glycolysis for energy compensation.<sup>[7]</sup> Combination therapy targeting both metabolic pathways has been exploited to increase the anticancer potency of single metabolic inhibitors,<sup>[8]</sup> but optimal proportion and toxic effects need to be settled before clinical studies. An alternative strategy may lie in targeting the signaling pathways that affect both mitochondrial and glycolytic metabolisms.<sup>[9]</sup> For example, to perturb mitochondrial and cytosolic redox homeostasis of cancer cells may induce oxidative stress, leading to mitochondrial dysfunction and glycolytic defect, and thereby to metabolic collapse and cell death.<sup>[10]</sup>

Thioredoxin reductase (TrxR) plays a pivotal role in defending reactive oxygen species (ROS) in cellular compartments,<sup>[11]</sup> which exists in three isoforms, that is, TrxR1 in cytosol, TrxR2 in mitochondria, and TrxR3 in testicles. Overexpression of TrxR in cancer cells has been related to drug resistances;<sup>[12]</sup> and TrxR has been demonstrated to influence cancer metabolic state via regulating cellular redox signaling pathways.<sup>[13]</sup> Moreover, TrxR2

specifically regulates redox status in mitochondria, and its inhibition may lead to a distinct pharmacodynamic profile.<sup>[14]</sup> Among TrxR inhibitors, metal complexes, such as those of Au, Ag, Ru or Ir, have been found to possess anticancer potency.<sup>[15,16]</sup> Some Pt complexes also showed strong inhibition to TrxR;<sup>[17]</sup> however, the perturbations of Pt-based TrxR inhibitors on energy metabolism are largely unknown.

Pt-based anticancer drugs, such as cisplatin (CDDP) and oxaliplatin, represent a class of successful metalodrugs in chemotherapy.<sup>[18]</sup> Nuclear genome is believed to be the main target for these drugs; however, their efficacy is often whittled away by DNA repair mechanisms.<sup>[19]</sup> Pt complexes with metabolism-inhibiting ability may circumvent this obstacle, but they suffered from metabolic alterations and discrepant effective doses between pharmacophores.<sup>[20,21]</sup> Interestingly, terpyridine Pt complexes could inhibit TrxR effectively,<sup>[22]</sup> thus providing a structural motif to accomplish synergistic inhibition to both mitochondrial and glycolytic metabolisms in cancer cells.

Triphenylphosphine (TPP) has been widely used as a mitochondrial targeting group, and TPP-tethered agents also showed potential to influence mitochondrial metabolism.<sup>[23,24]</sup> Herein we combined TPP and [(TPy)PtCl]<sup>+</sup> (TPy = 2,2':6',2''-terpyridine) to form a mitochondrion-targeted complex TTP (Figure 1) for the inhibition of mitochondrial TrxR. TTP causes tremendous damages to mitochondria, disturbs mitochondrial and cytosolic redox homeostasis, and destroys both respiratory and glycolytic phenotypes.

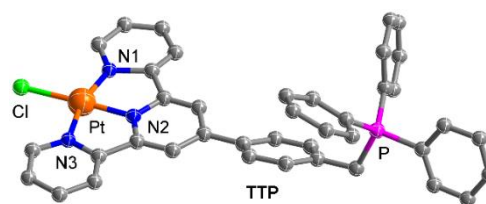


**Figure 1.** Crystal structure of TTP. Hydrogen atoms and chloride counter anions are omitted for clarity. Selected bond lengths (Å) and angles (°): N(1)-Pt 1.885(17), N(2)-Pt 1.971(15), N(3)-Pt 2.049(15), Cl-Pt 2.311(4); N(1)-Pt-N(2) 82.2(8), N(1)-Pt-N(3) 162.6(7), N(2)-Pt-N(3) 80.4(8), N(1)-Pt-Cl 98.0(6), N(2)-Pt-Cl 178.0(4), N(3)-Pt-Cl 99.4(5). Detailed data are deposited at the Cambridge Crystallographic Data Centre with the Deposition Number of CCDC 1573857.

[a] K. Wang, Dr. C. Zhu, Dr. Y. He, Dr. Z. Zhang, Dr. W. Zhou, Dr. N. Muhammad, Y. Guo, Prof. Dr. Z. Guo  
State Key Laboratory of Coordination Chemistry  
School of Chemistry and Chemical Engineering  
Nanjing University  
Nanjing 210023 (P. R. China)  
E-mail: zguo@nju.edu.cn

[b] Prof. Dr. X. Wang  
State Key Laboratory of Pharmaceutical Biotechnology  
School of Life Sciences  
Nanjing University  
Nanjing 210023 (P. R. China)  
E-mail: boxwxy@nju.edu.cn

## COMMUNICATION

membrane potential (30–60 mV) and large mitochondrial membrane potential (MMP) (140–180 mV) of cancer cells, being negative inside,<sup>[25]</sup> are expected to drive the dicationic lipophilic TTP to accumulate in mitochondria.

The cytotoxicity of TTP was tested by the MTT assay on a panel of human cancer cell lines, including Caov3 and SKOV3 (ovarian), HeLa (cervix), MCF-7 (breast), HCT-116 (colon), A549 and CDDP-resistant A549/DDP (lung), as well as normal cell line HK-2 (kidney), with CDDP as a reference. The half maximal inhibitory concentration (IC<sub>50</sub>) of TTP toward most of the tested cells is comparable to that of CDDP (Tables 1 and S3). Nevertheless, TTP showed an enhanced cytotoxicity against CDDP-insensitive Caov3 cells as compared to CDDP. Moreover, the ratio of IC<sub>50</sub> for A549 to that for A549/DDP (i.e. resistant factor) was decreased from 4.1 for CDDP to 2.5 for TTP, indicating that TTP can alleviate the drug resistance of A549 cells to CDDP. TTP was less toxic to normal HK-2 cells than CDDP, suggesting that it is much safer than CDDP as an anticancer agent.

**Table 1.** IC<sub>50</sub> values (μM) of TTP and CDDP for different cancer cell lines at 48 h. Data are shown as mean ± S.D. (n = 3).

Complex	Caov3	A549	A549/DDP	HK-2
TTP	9.0 ± 0.2	9.5 ± 1.2	24.1 ± 1.4	11.5 ± 0.6
CDDP	27.0 ± 1.3	5.9 ± 1.7	24.2 ± 1.3	7.0 ± 1.0

Cellular uptake and distribution of drug molecules are important factors for anticancer activity.<sup>[26]</sup> The Pt uptake in Caov3 cells was investigated using ICP-MS and shown in Table 2. It was reported that the Pt uptake is positively correlated with the cytotoxicity,<sup>[27]</sup> however, TTP demonstrated much higher cytotoxicity against Caov3 cells than CDDP though their total cellular uptake is similar. Since the Pt content in mitochondria of the TTP-treated cells is 2.65 times higher than that in the CDDP-treated cells, while that in nuclei is almost the same, the accumulation in mitochondria rather than the total cellular uptake seems to play a dominant role in the anticancer activity of TTP.

**Table 2.** Cellular distribution of Pt (ng μg<sup>-1</sup> protein) in Caov3 cells after incubation with TTP or CDDP (5 μM) at 37 °C for 24 h. Data are shown as mean ± S.D. (n = 3); blank values have been subtracted.

Complex	Mitochondria	Nuclei	Cytosol	Total
TTP	11.0 ± 0.2	13.5 ± 0.1	8.6 ± 0.1	33.2 ± 0.1
CDDP	4.2 ± 0.1	12.6 ± 0.2	12.4 ± 0.1	29.2 ± 0.1

The impact of TTP on DNA was first evaluated using calf-thymus DNA (CT-DNA). An immediate intercalation of TTP with DNA was observed in the UV-vis titration, and the affinity constant was calculated to be  $(1.30 \pm 0.07) \times 10^5 \text{ M}^{-1}$  (Figure S2). NaCl competitive experiment manifested that the interaction between TTP and CT-DNA is an electrostatic action (Figure S3). Hoechst 33342 staining was used to visualize the influence of TTP on nuclear DNA (nDNA) of Caov3 cells (Figure S4). After pre-incubation with TTP at its IC<sub>50</sub> for 24 h, almost no genome damage was observed. In the cell cycle assay, TTP-treated cells only showed a slightly increased S-phase arrest compared with

the control (Figure S5), suggesting that TTP caused little nDNA damage in Caov3 cells.

Mitochondria are essential for cancer formation and progression; and changes in mitochondrial morphology can determine the fate of cancer cells.<sup>[2]</sup> The effect of TTP on mitochondrial morphology in Caov3 cells was hence examined using transmission electron microscope (TEM). As shown in Figure 2, the mitochondria were induced into multilamellar globules and the folds of cristae in inner membrane extended to onion-like circles in the presence of TTP, indicating that mitochondria were severely damaged for cellular recycling. In contrast, the mitochondria in CDDP-treated cells remained almost unchanged. Immuno-fluorescence confirmed that TTP induced an increased expression of Mitofilin (IMMT) relevant to the regulation of cristae morphology (Figure S6),<sup>[28]</sup> providing a mechanism for the changes in mitochondrial morphology.

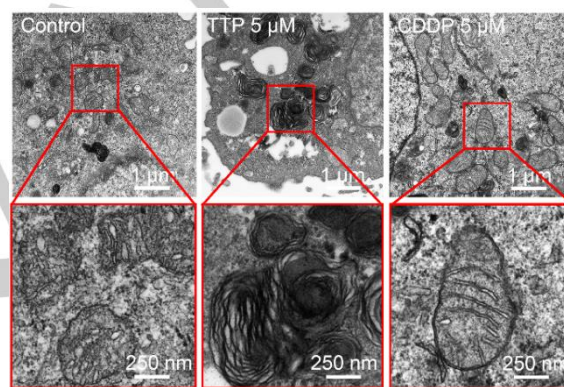


**Figure 2.** Typical TEM images indicating the alterations of mitochondrial morphology in Caov3 cells induced by TTP or CDDP at 37 °C for 48 h.

Mitochondrial damage may induce autophagy or mitophagy.<sup>[29]</sup> As an indicator of autophagy, formation of vacuoles was clearly visible in the TEM image upon treatment with TTP (Figure S7). Immunofluorescent assessment of LC3B showed that the fluorescence intensity and fluorescent dots increased in the TTP-treated Caov3 cells (Figure S8), manifesting that vacuoles of autophagosomes emerged. Further evidence of autophagy is shown in Figure 3. The ratio of lipidated LC3B-II to normal LC3B-I was increased after incubation with TTP, which is a reliable marker for autophagy.<sup>[29]</sup> The down-regulation of p62/SQSTM1 by TTP demonstrated that the protein was degraded in autophagosomes, which also verified the autophagic process of Caov3 cells.

Mitophagy was evaluated using TEM and confocal laser scanning microscopy. TEM images in Figure 4 (left) show that mitochondria are capped in the vacuoles, indicating that they were removed from cells through autophagosomes. The encapsulation of mitochondria in lysosomes is an important hallmark of mitophagy,<sup>[29]</sup> which was testified by co-localization of mitochondria and lysosomes. Remarkable overlap was observed in the confocal images of the TTP-treated Caov3 cells labelled by MitoTracker® Green FM and LysoTracker® Red DND-99 dyes

## COMMUNICATION

simultaneously; while no overlap was observed for the control. The results indicate that TTP could induce mitophagy.

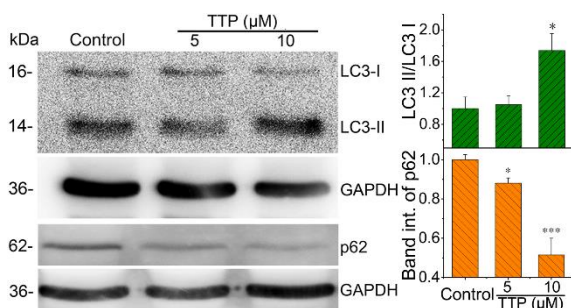


**Figure 3.** Immunoblotting of LC3B and p62 in Caov3 cells treated with TTP at 37 °C for 24 h and corresponding quantification of the LC3B-II to LC3B-I ratio and p62 expression. Error bars: S.D.,  $n = 3$ . Statistical significance of differences in mean values: \* $P < 0.05$ , \*\*\* $P < 0.001$ .

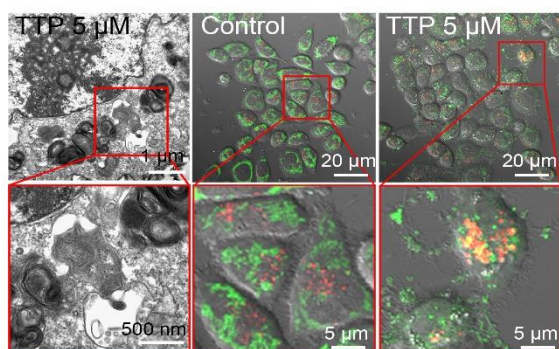


**Figure 4.** Representative TEM images of Caov3 cells treated with TTP at 37 °C for 48 h, emphasizing the region of mitophagy (left), and confocal microscopy images of Caov3 cells treated with TTP for 24 h (right).

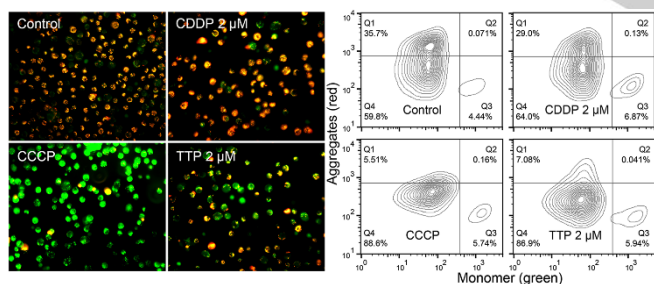


**Figure 5.** Fluorescent microscopy images (left) and flow cytometry quantification (right) of JC-1-labeled Caov3 cells treated with TTP or CDDP at 37 °C for 24 h ( $\lambda_{em} = 529, 590$  nm).

Dissipation of MMP is one of the important hallmarks of mitochondrial damage. The change of MMP was detected by JC-1, which aggregates to emit red fluorescence when MMP is high, and remains as monomers to emit green fluorescence when MMP is dissipated.<sup>[30]</sup> As shown in Figure 5, TTP-treated Caov3 cells emit green fluorescence, manifesting the dissipation of MMP. Flow cytometric analysis was also performed to identify

quantitatively the MMP in Caov3 cells. The data presented in Figure 5 by the contour plot illustrate that the fluorescence in Q1 for high MMP is shifted to Q4 for low MMP. For TTP-treated cells, the centres of contour plots assembled to one centre located in Q4 (86.9%), suggesting that TTP has a strong ability to dissipate the MMP, comparable to that of decoupler carbonyl cyanide 3-chlorophenyl hydrazone (CCCP, 88.6% in Q4). The results also suggest that the mitochondrial membrane was impaired by TTP.

Mitochondrial morphology is closely related to mitochondrial respiration,<sup>[31]</sup> which was evaluated using Seahorse Extracellular Flux analyser. Caov3 cells were pre-treated with TTP for 24 h before recording the oxygen consumption rate (OCR), with CDDP as a reference. As shown in Figure 6, TTP induced *ca* 50% decrease in both basal respiration and ATP production; moreover, it significantly destroyed the reverse capacity of the maximal oxygen consumption of the cells, which is indicated by the insensitive response to carbonylcyanide *p*-trifluoromethoxy phenylhydrazone (FCCP), an uncoupler of the proton gradient across the inner mitochondrial membrane. Mitochondrial respiration was shut down upon the injection of rotenone (an inhibitor of mitochondrial complex I) and antimycin A (an inhibitor of mitochondrial complex III) as the OCR decreased to minimum.<sup>[32]</sup> No significant change in OCR was detected for the CDDP-treated cells, indicating that CDDP hardly affects the mitochondrial respiration. Similar results were also found in A549 cell line (Figure S9A). Here, oligomycin was used to inhibit the ATP synthase and get the ATP synthetic ability of the cells.

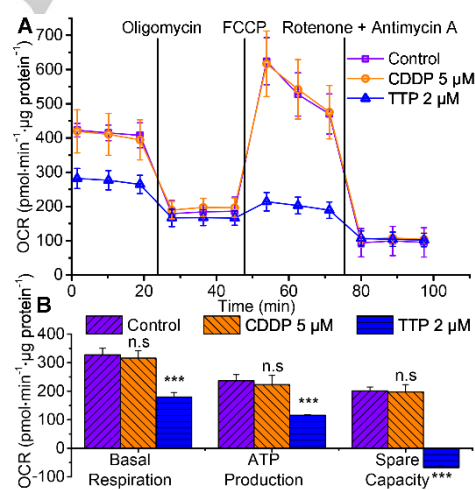


**Figure 6.** Kinetic profiles of OCR in Caov3 cells after treatment with TTP or CDDP at 37 °C for 24 h (A), and quantification of basal respiration, ATP production, and respiratory capacity from the kinetic profiles of OCR (B). Error bars: S.D.,  $n = 5$ . Statistical significance of differences in mean values: n.s. not significant, \*\*\* $P < 0.001$ .

The ATP production in Caov3 cells was further determined by the ATP assay kit (Figure S10). In the presence of TTP, ATP decreased in a dose-dependent way; while CDDP only induced a slight decrease in ATP. These results confirm that the mitochondrial basal respiration, ATP production capacity and respiratory capacity were severely damaged by TTP. However,

## COMMUNICATION

the activity of ATP synthase was only marginally affected by TTP (Figure S11), so ATP synthase is unlikely to be the main target of TTP. The significant decrease in ATP production may arise from the dysfunction of mitochondria due to morphological disruptions.

Destruction of mitochondrial metabolism could influence the intracellular redox homeostasis,<sup>[10]</sup> so ROS production was tracked with flow cytometry by recording the fluorescence of 2',7'-dichlorodihydrofluorescein oxidized from 2',7'-dichlorofluorescein diacetate. In the presence of TTP, the cellular ROS production decreased ca 30%, and the mitochondrial superoxide (mtSOX), a byproduct of mitochondrial respiration,<sup>[33]</sup> also decreased moderately compared to the control (Figure S12), highlighting an obvious interference in redox homeostasis; on the contrary, CDDP induced a moderate increase in both cellular ROS and mtSOX. These results imply that the cellular ROS-defensive systems were damaged by TTP.

TrxR systems play an important role in regulating diverse cellular redox events,<sup>[13]</sup> and defects in TrxR2 were reported to induce collapse in mitochondrial cristae and respiration.<sup>[34]</sup> We thus evaluated the effects of TTP on the mitochondrial and cellular TrxR activities. The activity of purified TrxR for 5,5'-dithio-bis-(2-nitrobenzoic acid) was dramatically inhibited by TTP ( $IC_{50} = 74$  nM), which is more potent than CDDP ( $IC_{50} > 1000$  nM) (Figure 7A and S13). Further, TTP-treated Caov3 cells were lysed to evaluate the effects of TTP on mitochondrial and cellular TrxR. As shown in Figure 7B, TTP significantly reduced the activity of mitochondrial and cellular TrxR by 70% and 50% respectively; whereas CDDP moderately inhibited the activity. Cysteine and selenocysteine were used to understand the reaction of TrxR with TTP.<sup>[35]</sup> Significant chemical shifts were observed in the <sup>1</sup>H NMR spectra for the reaction within 10 min (Figure S14), implying that TTP may readily react with these residues in TrxR. These results show that TrxR is the most probable molecular target for TTP to induce mitochondrial changes and affect their functions.

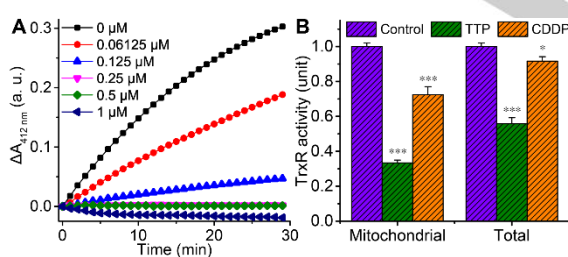


**Figure 7.** Inhibition of the activity of purified TrxR by TTP (A), and quantification of mitochondrial and total TrxR activity in Caov3 cells treated with TTP or CDDP (10  $\mu$ M) at 37  $^{\circ}$ C for 24 h (B). Error bars: S.D., n = 3. Statistical significance of differences in mean values: \*P < 0.05, \*\*\*P < 0.001.

Inhibition or depletion of TrxR2 was shown to abrogate the expression of activated caspase-3, a key mediator of both mitochondrial and nuclear events of apoptosis.<sup>[36]</sup> The expression of activated caspase-3 in Caov3 cells was evaluated by Western blot. Little activated caspase-3 was observed for the TTP-treated cells; while evident activated caspase-3 band was observed for the CDDP-treated cells (Figure S15), indicating apoptosis had occurred. The results manifest that Caov3 cells died via a

caspase-3-independent non-apoptosis pathway,<sup>[37]</sup> which further confirmed the strong inhibition of TrxR2 by TTP.

Although mitochondrial respiration is strongly suppressed by TTP, cancer cells are metabolically flexible. Simultaneous inhibition of glycolysis may restrain the energy production and cut off the metabolites for mitochondrial respiration.<sup>[9,38]</sup> Therefore, extracellular acidification rate (ECAR) in Caov3 cells was measured, which reflects the glycolytic capacity of the cells. As shown in Figure 8A, TTP induced ca 50% decrease in basal ECAR compared to the control, indicating that the glycolytic capacity was remarkably inhibited; while CDDP barely influenced the basal glycolysis. The maximum ECAR for TTP- and CDDP-treated cells determined at the steady state (42 min) are almost the same as the control. The basal ECAR of TTP-treated A549 cells decreased ca 85% (Figure S9B), which further confirmed the suppression of glycolytic capacity by TTP. The OCR vs ECAR profile provides a more comprehensive understanding on bioenergetics and reflects the contribution of two major pathways to energy production.<sup>[32]</sup> As shown in Figure 8B, TTP led to dramatic decreases in both OCR and ECAR, indicating that mitochondrial and glycolytic metabolisms were reduced simultaneously to give a hypometabolic state; while CDDP induced the cells to stay at a hypermetabolic state. One of the big challenges for metabolic inhibition therapy lies in the metabolic heterogeneity within tumor cells; so drugs that target multiple metabolic phenotypes are attractive for chemotherapy.<sup>[9]</sup> TTP possesses the potential to inhibit both mitochondrial and glycolytic metabolisms, thereby blocking the brisk metabolic adaption of tumor cells, which may pave a new way for the design of novel platinum-based drugs.

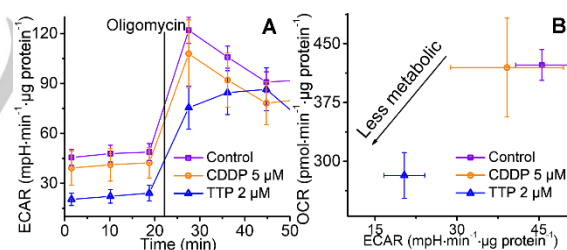


**Figure 8.** Kinetic profiles of ECAR in Caov3 cells after treatment with TTP or CDDP at 37  $^{\circ}$ C for 24 h (A), and indices of cancer metabolism degree calculated from OCR and ECAR profiles of Caov3 cells (B).

In summary, a mitochondrion-targeted Pt(II) complex (TTP) was developed to disrupt mitochondrial structure and suppress mitochondrial TrxR2 of cancer cells. The mitochondrial morphology and function are severely damaged, and the mitochondrial and glycolytic metabolisms are significantly impaired by TTP. Cancer cells are flexible and often adapt their metabolic phenotypes for abnormal microenvironment to satisfy their growth needs. Targeted therapy for multiple metabolic phenotypes is a promising strategy to address this issue.<sup>[9]</sup> TTP inhibits mitochondrial respiration and glycolysis simultaneously through regulating the TrxR systems, thereby making cancer cells get into a hypometabolic phenotype and starving them to death. This work highlights the pleiotropic effects of a metallodrug on the

## COMMUNICATION

energy metabolism of cancer cells and proves that targeting redox homeostasis is an effective way for modulating metabolic pathways relevant to cancer development. Nevertheless, some off-target effects may occur to this strategy; how to mitigate such risks still remains to be a challenge in the future.

## Acknowledgements

We are grateful to the National Natural Science Foundation of China (Grants 31700714, 31570809, 21877059), the National Basic Research Program of China (Grants 2015CB856300) and National Science Foundation of Jiangsu Province (Grant BK20150054) for financial support.

**Keywords:** anticancer drug • platinum(II) complex • mitochondrion • metabolism • thioredoxin reductase

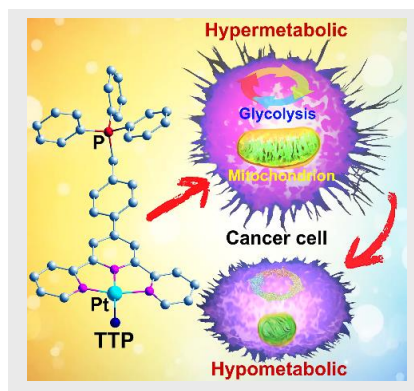
- [1] O. Warburg, *Science* **1956**, *124*, 269-270.
- [2] D. C. Wallace, *Nat. Rev. Cancer* **2012**, *12*, 685-698.
- [3] P. E. Porporato, N. Filigheddu, J. Pedro, G. Kroemer, L. Galluzzi, *Cell Res.* **2018**, *28*, 265-280.
- [4] S. E. Weinberg, N. S. Chandel, *Nat. Chem. Biol.* **2015**, *11*, 9-15.
- [5] P. Y. Zhang, C. Chiu, H. Y. Huang, Y. Lam, A. Habtemariam, T. Malcomson, M. J. Paterson, G. J. Clarkson, P. B. O'Connor, H. Chao, P. J. Sadler, *Angew. Chem. Int. Ed.* **2017**, *56*, 14898-14902; *Angew. Chem.* **2017**, *129*, 15094-15098.
- [6] J. J. Cao, C. P. Tan, M. H. Chen, N. Wu, D. Y. Yao, X. G. Liu, L. N. Ji and Z. W. Mao, *Chem. Sci.* **2017**, *8*, 631-640.
- [7] A. Schulze, A. L. Harris, *Nature* **2012**, *491*, 364-373.
- [8] J. Liu, C. Jin, B. Yuan, Y. Chen, X. Liu, L. Ji, H. Chao, *Chem. Commun.* **2017**, *53*, 9878-9881.
- [9] U. E. Martinez-Outschoorn, M. Peiris-Pages, R. G. Pestell, F. Sotgia, M. P. Lisanti, *Nat. Rev. Clin. Oncol.* **2017**, *14*, 11-31.
- [10] C. Gorrini, I. S. Harris, T. W. Mak, *Nat. Rev. Drug Discov.* **2013**, *12*, 931-947.
- [11] J. Nordberg, E. S. Arner, *Free Radic. Biol. Med.* **2001**, *31*, 1287-1312.
- [12] D. T. Lincoln, E. E. Ali, K. F. Tonissen, F. M. Clarke, *Anticancer Res.* **2003**, *23*, 2425-2433.
- [13] J. M. Zhang, X. M. Li, X. Han, R. J. Liu, J. G. Fang, *Trends Pharmacol. Sci.* **2017**, *38*, 794-808.
- [14] O. Rackham, A. M. Shearwood, R. Thyer, E. McNamara, S. M. Davies, B. A. Callus, A. Miranda-Vizuete, S. J. Berners-Price, Q. Cheng, E. S. Arner, A. Filipovska, *Free Radic. Biol. Med.* **2011**, *50*, 689-699.
- [15] Y. Z. Cheng, Y. Qi, *Anticancer Agents Med. Chem.* **2017**, *17*, 1046-1069.
- [16] T. T. Zou, C. T. Lum, C. N. Lok, W. P. To, K. H. Low, C. M. Che, *Angew. Chem. Int. Ed.* **2014**, *53*, 5810-5814; *Angew. Chem.* **2014**, *126*, 5920-5924.
- [17] R. Ahmadi, S. Urig, M. Hartmann, B. M. Helmke, S. Koncarevic, B. Allenberger, C. Kienhoefer, M. Neher, H. H. Steiner, A. Unterberg, C. Herold-Mende, K. Becker, *Free Radic. Biol. Med.* **2006**, *40*, 763-778.
- [18] T. C. Johnstone, K. Suntharalingam, S. J. Lippard, *Chem. Rev.* **2016**, *116*, 3436-3486.
- [19] M. Kartalou, J. M. Essigmann, *Mutat. Res.* **2001**, *478*, 1-21.
- [20] J. Zajac, H. Kostrhunova, V. Novohradsky, O. Vrana, R. Raveendran, D. Gibson, J. Kasparkova, V. Brabec, *J. Inorg. Biochem.* **2016**, *156*, 89-97.
- [21] S. Dhar, S. J. Lippard, *Proc. Natl. Acad. Sci. USA* **2009**, *106*, 22199-22204.
- [22] K. Becker, C. Herold-Mende, J. J. Park, G. Lowe, R. H. Schirmer, *J. Med. Chem.* **2001**, *44*, 2784-2792.
- [23] S. X. Jin, Y. Hao, Z. Z. Zhu, N. Muhammad, Z. Q. Zhang, K. Wang, Y. Guo, Z. J. Guo, X. Y. Wang, *Inorg. Chem.* **2018**, *57*, 11135-11145.
- [24] J. Zielonka, J. Joseph, A. Sikora, M. Hardy, O. Ouari, J. Vasquez-Vivar, G. Cheng, M. Lopez, B. Kalyanaraman, *Chem. Rev.* **2017**, *117*, 10043-10120.
- [25] M. P. Murphy, R. A. Smith, *Annu. Rev. Pharmacol. Toxicol.* **2007**, *47*, 629-656.
- [26] A. V. Klein, T. W. Hambley, *Chem. Rev.* **2009**, *109*, 4911-4920.
- [27] Z. H. Siddik, *Oncogene* **2003**, *22*, 7265-7279.
- [28] R. M. Zerbes, I. J. van der Klei, M. Veenhuis, N. Pfanner, M. van der Laan, M. Bohnert, *Biol. Chem.* **2012**, *393*, 1247-1261.
- [29] D. J. Klionsky, F. C. Abdalla, H. Abeliovich et al., *Autophagy* **2012**, *8*, 445-544.
- [30] S. T. Smiley, M. Reers, C. Mottola-Hartshorn, M. Lin, A. Chen, T. W. Smith, G. J. Steele, L. B. Chen, *Proc. Natl. Acad. Sci. USA* **1991**, *88*, 3671-3675.
- [31] L. Plecita-Hlavata, H. Engstova, L. Alan, T. Spacek, A. Dlaskova, K. Smolkova, J. Spackova, J. Tauber, V. Stradalova, J. Malinsky, M. Lessard, J. Bewersdorf, P. Jezek, *Faseb J.* **2016**, *30*, 1941-1957.
- [32] D. A. Ferrick, A. Neilson, C. Beeson, *Drug Discov. Today* **2008**, *13*, 268-274.
- [33] P. Venditti, L. Di Stefano, S. Di Meo, *Mitochondrion* **2013**, *13*, 71-82.
- [34] V. Scalcon, A. Bindoli, M. P. Rigobello, *Free Radic. Biol. Med.* **2018**, *127*, 62-79.
- [35] J. L. Hickey, R. A. Ruhayel, P. J. Barnard, M. V. Baker, S. J. Berners-Price, A. Filipovska, *J. Am. Chem. Soc.* **2008**, *130*, 12570-12571.
- [36] M. Benhar, M. T. Forrester, D. T. Hess, J. S. Stamler, *Science* **2008**, *320*, 1050-1054.
- [37] S. A. Lakhani, A. Masud, K. Kuida, G. J. Porter, C. J. Booth, W. Z. Mehal, I. Inayat, R. A. Flavell, *Science* **2006**, *311*, 847-851.
- [38] J. Zheng, *Oncol. Lett.* **2012**, *4*, 1151-1157.

## COMMUNICATION

## Entry for the Table of Contents

## COMMUNICATION

A triphenylphosphonium-modified terpyridine platinum(II) complex exhibits enhanced cytotoxicity against human ovarian cancer cells, and shows strong inhibitory effects on both mitochondrial and glycolytic metabolisms, inducing the cells to enter into a hypometabolic state.



Kun Wang, Chengcheng Zhu, Yafeng He, Zhenqin Zhang, Wen Zhou, Nafees Muhammad, Yan Guo, Xiaoyong Wang,\* and Zijian Guo\*

Page No. – Page No.

Restraining Cancer Cells by Dual-Metabolic Inhibitions with a Mitochondrion-Targeted Platinum(II) Complex